FREE VIBRATIONS OF THE VISCOELASTIC HUMAN SKULL

A. Charalambopoulos, D.I. Fotiadis and C.V. Massalas

12-97

Preprint no. 12-97/1997

Department of Computer Science
University of Ioannina
451 10 Ioannina, Greece

FREE VIBRATIONS OF THE VISCOELASTIC HUMAN SKULL

A. CHARALAMBOPOULOS

Inst. of Chemical Engineering and High Temperature Chemical Processes, GR 26500 Patras, Greece

D.I. FOTIADIS

Dept. of Computer Science, Univ. of Ioannina, GR 45110 Ioannina, Greece

and

C.V. MASSALAS

Dept. of Mathematics, Univ. of Ioannina, GR 45110 Ioannina, Greece

SUMMARY

In this work we deal with the free vibrations of a viscoelastic skull. The analysis is based on the three-dimensional theory of viscoelasticity and the representation of the displacement field in terms of the Navier eigenvectors. The frequency equation was solved numerically and results are presented for the eigenfrequency and the attenuation spectra.

1. INTRODUCTION

Several investigators have studied the frequency spectrum of the human skull both theoretically and experimentally. It is well known that the knowledge of the frequency spectrum can be applied for better understanding of head injuries and in the diagnosis of head diseases. One subject which attracted the attention of many researchers is the free vibration analysis of the human skull. From the experimental point of view, Khalil et al. [1] have presented experimental measurements for the resonance frequencies of the human skull for two kinds of dry skulls and extrapolated their results to living skulls taking into account known and estimated differences in mechanical properties. Håkansson et al. [2] investigated the free damped natural frequencies of the human skull *in vivo* and they are the only ones to our knowledge who reported damping coefficients.

In previous communications we have studied the dynamic characteristics of the human dry skull [3], as well as the effect of various geometrical parameters on them [4,5]. We restricted our study to the sensitivity of the frequency spectrum from the various parameters assuming that the skull is a linear isotropic elastic material. Several other researchers have paid attention to the dissipative material behaviour of the human head system. Misra [6] studied the steady - state response of a prolate spheroidal shell made of a linear viscoelastic solid containing a viscoelastic fluid due to an axisymmetric load varying harmonically with time. Misra and Chakravarty [7] have shown that the dissipative material of the skull as well as the brain have a significant effect on the frequency spectrum of the freely vibrating cranial system. The three - dimensional equations of linear viscoelasticity have been used by Hickling et al. [8] to describe the behaviour of both the brain and the skull to an axisymmetric impact. However, in the above works no clear statement has been done about the cause of dissipative behaviour of the human head system which matches qualitatively the results of Håkansson et al. [2].

In the present work we deal with the role of material behaviour on the frequency spectrum of the human skull. The mathematical modelling is based on the three-dimensional theory of elasticity and the approximation of the skull by a linear viscoelastic material occupying the region bounded by two concentric spheres. We assume steady vibrations with angular frequency ω_1 and attenuation ω_2 and taking advantage of the Fourier transform properties we obtain the variables which replace

Lamè's constants of the elastic material case. The mathematical analysis is based on the representation of the displacement field in terms of the Navier eigenvectors. The frequency equation is constructed by imposing the satisfaction of the boundary conditions and it is solved numerically. Due to the existence of complex terms this leads to zero-crossing finding of two functions in the complex plane. From the analysis adopted we obtained ω_1^m and ω_2^m, $m = 1,2,3,...$ for real and complex ν (Poisson's ratio) and we also performed a sensitivity analysis of our results for various parameters entering the problem.

2. PROBLEM FORMULATION

We consider two concentric spheres with center 0, radii r_0, r_1 and surfaces S_0, S_1 respectively (Fig. 1).

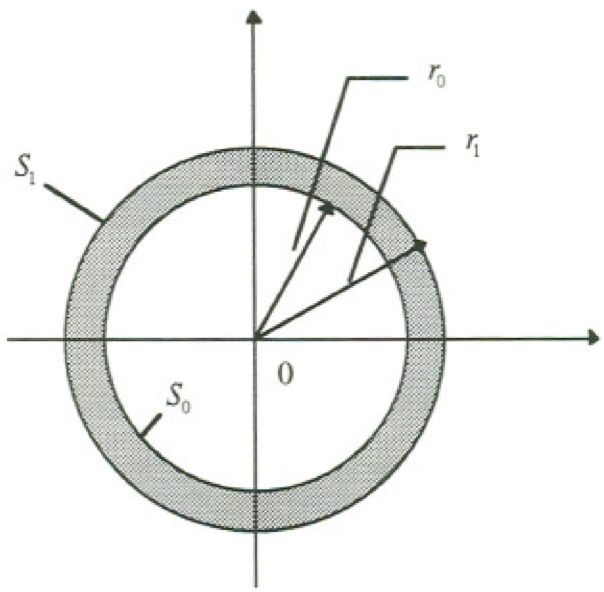

Figure 1: Problem Geometry

The region V between the two spheres is assumed to be filled with a viscoelastic material obeying to the following constitutive equation

$$\bar{\tau}(\boldsymbol{r},t) = \int_{-\infty}^{t} \left\{ \begin{matrix} G_1(t-\tau)\dfrac{1}{2}\dfrac{\partial}{\partial\tau}\left[\nabla\boldsymbol{u}(\boldsymbol{r},\tau) + (\nabla\boldsymbol{u}(\boldsymbol{r},\tau))^T\right] + \\ \dfrac{1}{3}\{G_2(t-\tau) - G_1(t-\tau)\}\dfrac{\partial}{\partial\tau}(\nabla\cdot\boldsymbol{u}(\boldsymbol{r},\tau))\boldsymbol{I} \end{matrix} \right\} d\tau \tag{1}$$

where $\boldsymbol{u}$ stands for the displacement vector of the viscoelastic medium, $\bar{\tau}(\boldsymbol{r},t)$ the stress tensor, $\boldsymbol{I}$ the identity tensor and $G_1(\xi), G_2(\xi)$ are independent functions, having zero values for negative argument and defining the viscoelastic properties of the medium.

The kinematic behaviour of the system is described by the equation

$$\tau_{ij,j} = \rho \ddot{u}_i, \quad i,j = 1,2,3 \tag{2}$$

where indices indicate components of the corresponding tensors while indices after the comma indicate differentiation with respect to the corresponding cartesian coordinate.

Assuming steady vibrations of the system under consideration, with angular frequency ω_1 and attenuation (due to viscous properties) ω_2 we apply Fourier transform analysis to the problem defining

$$\hat{\boldsymbol{u}}(\boldsymbol{r},\omega) = \int_{-\infty}^{+\infty} \boldsymbol{u}(\boldsymbol{r},t) e^{-i\omega t} dt \tag{3}$$

$$\bar{\tau}(\boldsymbol{r},\omega) = \int_{-\infty}^{+\infty} \tau(\boldsymbol{r},\omega) e^{-i\omega t} dt \tag{4}$$

and

$$g_j(\omega) = \int_{0}^{+\infty} G_j(t) e^{-i\omega t} dt, \quad j = 1,2 \tag{5}$$

with $\omega = \omega_1 + i\omega_2$.

Combining (1), (2), (3), (4), (5) and taking advantage of Fourier transform properties we obtain

$$\frac{1}{2} i\omega g_1(\omega)\left[\nabla^2 \hat{\boldsymbol{u}}(\boldsymbol{r},\omega) + \nabla(\nabla \cdot \hat{\boldsymbol{u}}(\boldsymbol{r},\omega))\right] +$$
$$\frac{1}{3} i\omega\left[g_2(\omega) - g_1(\omega)\right]\nabla(\nabla \cdot \hat{\boldsymbol{u}}(\boldsymbol{r},\omega)) + \rho\omega^2 \hat{\boldsymbol{u}}(\boldsymbol{r},\omega) = \boldsymbol{0}$$

or

$$G^*(\omega)\nabla^2\hat{\boldsymbol{u}} + \left[G^*(\omega) + \lambda^*(\omega)\right]\nabla(\nabla\cdot\hat{\boldsymbol{u}}) + \rho\omega^2\hat{\boldsymbol{u}} = \boldsymbol{0} \tag{6}$$

where

$$G^*(\omega) = \frac{1}{2}i\omega g_1(\omega) \tag{7}$$

$$\lambda^*(\omega) = \frac{1}{3}i\omega\left[g_2(\omega) - g_1(\omega)\right] \tag{8}$$

are the frequency functions replacing Lamè's constants μ, λ, respectively, in the case of elastic materials.

It is convenient to express $G^*(\omega)$, $\lambda^*(\omega)$ in terms of the generalised Young's modulus $E(\omega) = i\omega g_1\dfrac{3g_2}{g\ +2g_2}$ and the Poisson's ratio $\nu(\omega) = \dfrac{g_2(\omega) - g_1(\omega)}{g_1(\omega) + 2g_2(\omega)}$ through the relations $G^*(\omega) = \dfrac{E(\omega)}{2(1+\nu(\omega))}$ and $\lambda^*(\omega) = \dfrac{E(\omega)\nu(\omega)}{(1+\nu(\omega))(1-2\nu(\omega))}$.

So, in the frequency domain, the viscoelastic properties of the medium under consideration are completely described by the functions $E(\omega)$, $\nu(\omega)$.

Inserting dimensionless variables the equation of elasticity (6) takes the form

$$\tilde{G}^*(\omega)\nabla'^2\hat{\boldsymbol{u}}(\boldsymbol{r}') + \left[G^*(\omega) + \lambda^*(\omega)\right]\nabla'(\nabla'\cdot\hat{\boldsymbol{u}}(\boldsymbol{r}')) + \Omega^2\hat{\boldsymbol{u}}(\boldsymbol{r}') = \boldsymbol{0} \tag{9}$$

where

$\boldsymbol{r}' = \boldsymbol{r}/\alpha$ $(\alpha = r_1)$, $\nabla' = \alpha\nabla$, $\tilde{G}^*(\omega) = G^*(\omega)/G^*(\omega) = 1$,

$\tilde{\lambda}^*(\omega) = \lambda^*(\omega)/G^*(\omega) = 2\nu(\omega)/(1-2\nu(\omega))$, $\Omega = \omega\alpha\sqrt{2\rho(1+\nu(\omega))/E(\omega)}$.

In equation (9) the indication of the dependence of $\hat{\boldsymbol{u}}(r,\omega)$ with respect to ω has been for simplicity suppressed.

The physical characteristics of the system enter the mathematical formulation of the problem through the boundary conditions that are described on surfaces S_0, S_1. More precisely these two surfaces are stress free, that is

$$\boldsymbol{T}\boldsymbol{u}(\boldsymbol{r}') = 0, \quad \boldsymbol{r}' \in S_0, \ S_1 \tag{10}$$

where

$$\boldsymbol{T} = 2\tilde{G}^*(\omega)\hat{\boldsymbol{r}}' \cdot \nabla' + \tilde{\lambda}^*(\omega)\hat{\boldsymbol{r}}(\nabla' \cdot) + \tilde{G}^*(\omega)\hat{\boldsymbol{r}} \times \nabla' \times \tag{11}$$

stands for the dimensionless surface stress operator in the medium V, $\hat{\boldsymbol{r}}$ is the unit normal vector on surfaces S_0, S_1, and

$$\mu' = \frac{G^*(\omega)}{G^*(\omega)} = 1 \tag{12}$$

$$\lambda' = \frac{\lambda^*(\omega)}{G^*(\omega)} = \frac{2\nu(\omega)}{1 - 2\nu(\omega)}. \tag{13}$$

We note that, the system of equations (6) - (10) constitutes a well - posed "corresponding" problem. With this term is meant the identical problem except that the body concerned is viscoelastic instead of elastic.

The method adopted for the solution of this problem is based on the representation of the displacement field $\boldsymbol{u}(\boldsymbol{r})$ in terms of the Navier eigenvectors [9]. As it is well known, Navier eigenvectors are created through Helmholtz decomposition and constitute of a complete set of vector functions in the space of solutions of the time-independent Navier equation.

The Navier eigenvectors have the following form

$$\boldsymbol{L}_n^{m,l}(\boldsymbol{r}') = \dot{g}_n^l(\Omega r')\boldsymbol{P}_n^m(\hat{\boldsymbol{r}}) + \sqrt{n(n+1)}\frac{g_n^l(\Omega r')}{\Omega r'}\boldsymbol{B}_n^m(\hat{\boldsymbol{r}}) \tag{14}$$

$$\boldsymbol{M}_n^{m,l}(\boldsymbol{r}') = \sqrt{n(n+1)}g_n^l(k'_s r')\boldsymbol{C}_n^m(\hat{\boldsymbol{r}}) \tag{15}$$

$$N_n^{m,l}(\boldsymbol{r}') = n(n+1)\frac{g_n^l(k'_s r')}{k'_s r'}\boldsymbol{P}_n^m(\hat{\boldsymbol{r}}) +$$
$$\sqrt{n(n+1)}\left[\dot{g}_n^l(k'_s r') + \frac{g_n^l(k'_s r')}{k'_s r'}\right]\boldsymbol{B}_n^m(\hat{\boldsymbol{r}}) \tag{16}$$

$n = 0,1,2,\ldots;\ \ m = -n,-n+1,\ldots,n-1,n;\ \ l = 1,2$

where

$$k'_s = \frac{\Omega}{\tilde{G}^{*1/2}} \tag{17}$$

$$g_n^l(x) = \begin{cases} J_n(x) & l = 1 \quad \text{(spherical Bessel function of order } n\text{)} \\ Y_n(x) & l = 2 \quad \text{(spherical Neumann function of order } n\text{)} \end{cases} \tag{18}$$

where $\dot{g}_n^l(x)$ stands for the derivative of $g_n^l(x)$ with respect to its argument. Finally, the functions $\boldsymbol{P}_n^m(\hat{\boldsymbol{r}})$, $\boldsymbol{B}_n^m(\hat{\boldsymbol{r}})$, $\boldsymbol{C}_n^m(\hat{\boldsymbol{r}})$ defined on the unit sphere, are the vector spherical harmonics, introduced by Hansen [9] and are given by the relations

$$\boldsymbol{P}_n^m(\hat{\boldsymbol{r}}) = \hat{\boldsymbol{r}}Y_n^m(\hat{\boldsymbol{r}}) \tag{19}$$

$$\boldsymbol{B}_n^m(\hat{\boldsymbol{r}}) = \frac{1}{\sqrt{n(n+1)}}\left[\hat{\vartheta}\frac{\partial}{\partial\vartheta} + \frac{\hat{\varphi}}{\sin\vartheta}\frac{\partial}{\partial\varphi}\right]Y_n^m(\hat{\boldsymbol{r}}) \tag{20}$$

$$\boldsymbol{C}_n^m(\hat{\boldsymbol{r}}) = \frac{1}{\sqrt{n(n+1)}}\left[\frac{\hat{\vartheta}}{\sin\vartheta}\frac{\partial}{\partial\varphi} - \hat{\varphi}\frac{\partial}{\partial\vartheta}\right]Y_n^m(\hat{\boldsymbol{r}}) \tag{21}$$

where $Y_n^m(\hat{\boldsymbol{r}}) = P_n^m(\cos\vartheta)e^{im\varphi}$ are the spherical harmonics and $P_n^m(\cos\vartheta)$ the well known Legendre functions.

Consequently the displacement field $\boldsymbol{u}(\boldsymbol{r})$ has the representation

$$\boldsymbol{u}(\boldsymbol{r}) = \sum_{n=0}^{+\infty}\sum_{m=-n}^{n}\sum_{l=1}^{2}\left\{\alpha_n^{m,l}\boldsymbol{L}_n^{m,l}(\boldsymbol{r}) + \beta_n^{m,l}\boldsymbol{M}_n^{m,l}(\boldsymbol{r}) + \gamma_n^{m,l}\boldsymbol{N}_n^{m,l}(\boldsymbol{r})\right\}. \tag{22}$$

Now, the problem of the determination of $\boldsymbol{u}(\boldsymbol{r})$ is transferred to the determination of the coefficients of the expansion (22) in Navier eigenfunctions. The expression (22) satisfies Navier equation. What remains to do is to force this expansion to satisfy the boundary conditions (10). Consequently applying the stress operator $\boldsymbol{T}$ on the expansion (22), expressing the functions $\boldsymbol{TL}_n^{m,l}$, $\boldsymbol{TM}_n^{m,l}$, $\boldsymbol{TN}_n^{m,l}$ in terms of the orthogonal set of vector harmonics $\boldsymbol{P}_n^m$, $\boldsymbol{B}_n^m$, $\boldsymbol{C}_n^m$ and taking advantage of the independence of the last functions we conclude that for every specific pair of integers (n,m), with $|m| \le n$ the six coefficients involved in expansion (22) satisfy a linear homogeneous system of six equations of the form

$$\boldsymbol{D}_n^m \boldsymbol{x}_n^m = \boldsymbol{0} \tag{23}$$

where

$$\boldsymbol{x}_n^m = \left[\alpha_n^{m,1}, \alpha_n^{m,2}, \beta_n^{m,1}, \beta_n^{m,2}, \gamma_n^{m,1}, \gamma_n^{m,2}\right]^T$$

and

$$\boldsymbol{D}_n^m = \begin{bmatrix} A_n^1(r'_1) & A_n^2(r'_1) & 0 & 0 & D_n^1(r'_1) & D_n^2(r'_1) \\ 0 & 0 & C_n^1(r'_1) & C_n^2(r'_1) & 0 & 0 \\ B_n^1(r'_1) & B_n^2(r'_1) & 0 & 0 & E_n^1(r'_1) & E_n^1(r'_1) \\ A_n^1(r'_0) & A_n^2(r'_0) & 0 & 0 & D_n^1(r'_0) & D_n^2(r'_0) \\ 0 & 0 & C_n^l(r'_0) & C_n^l(r'_0) & 0 & 0 \\ B_n^1(r'_0) & B_n^2(r'_0) & 0 & 0 & E_n^1(r'_0) & E_n^2(r'_0) \end{bmatrix}$$

where

$$A_n^l(r') = -\left[\frac{4}{r'}\dot{g}_n^l(\Omega r') + 2\Omega\left(1 - \frac{n(n+1)}{\Omega^2 r'^2}\right)g_n^l(\Omega r') + \lambda'\,\Omega g_n^l(\Omega r')\right],$$

$$B_n^l(r') = 2\sqrt{n(n+1)}\left[\dot{g}_n^l(\Omega r')\frac{1}{r'} - \frac{g_n^l(\Omega r')}{\Omega r'^2}\right],$$

$$C_n^l(r') = \sqrt{n(n+1)}\left[(2+\lambda')^{1/2}\Omega\dot{g}_n^l((2+\lambda')^{1/2}\Omega r') - \frac{1}{r'}g_n^l((2+\lambda')^{1/2}\Omega r')\right],$$

$$D_n^l(r') = 2n(n+1)\left[\frac{\dot{g}_n^l((2+\lambda')^{1/2}\Omega r')}{r'} - \frac{g_n^l((2+\lambda')^{1/2}\Omega r')}{(2+\lambda')^{1/2}\Omega r'}\right],$$

$$E_n^l(r') = \sqrt{n(n+1)}\left[\begin{array}{l} -2\dfrac{\dot{g}_n^l((2+\lambda')^{1/2}\Omega r')}{r'} - (2+\lambda')^{1/2}\Omega g_n^l((2+\lambda')^{1/2}\Omega r') \\ +2\dfrac{n(n+1)-1}{(2+\lambda')^{1/2}\Omega r'^2} g_n^l((2+\lambda')^{1/2}\Omega r') \end{array}\right].$$

In order for the system (23) to have a nontrivial solution the following condition must be satisfied

$$\det\left(\boldsymbol{D}_n^m(\Omega)\right) = 0. \tag{24}$$

This condition provides the characteristic (frequency) equation from the roots of which we obtain the eigenfrequencies ω_1^m and the attenuation coefficients ω_2^m, $m = 1,2,3,...$, of the system under discussion.

3. SOLUTION - NUMERICAL RESULTS

The frequency equation (24) is treated numerically in order its solution $\Omega^m = \Omega_1^m + i\Omega_2^m$ to be obtained. The spherical Bessel functions and their derivatives for complex arguments are computed using backward recurrence. The spherical Neumann functions and their derivatives are computed using a mixed recurrence because its value decreases first and increases as its order increases [10]. A complex LU - decomposition routine is used along with a determinant computation routine which results in the following

$$\mathrm{Re}\left[\det\left(\boldsymbol{D}_n^m(\Omega)\right)\right] + i\,\mathrm{Im}\left[\det\left(\boldsymbol{D}_n^m(\Omega)\right)\right] = 0 \tag{25}$$

or

$$\mathrm{Re}\left[\det\left(\boldsymbol{D}_n^m(\Omega_1,\Omega_2)\right)\right] + i\,\mathrm{Im}\left[\det\left(\boldsymbol{D}_n^m(\Omega_1,\Omega_2)\right)\right] = 0 \tag{26}$$

which is equivalent to

$$\mathrm{Re}\left[\det\left(\boldsymbol{D}_n^m(\Omega_1,\Omega_2)\right)\right] = 0 \tag{27a}$$

$$\mathrm{Im}\left[\det\left(\boldsymbol{D}_n^m(\Omega_1,\Omega_2)\right)\right]=0. \quad (27b)$$

The solution of the system of equations (27) is obtained by a bisection grid method. A rectangular grid is established in the (Ω_1,Ω_2) plane and bisection searches for zero crossings are done along each of the equally spaced grid lines. The spacing chosen for the present solution is 10^{-3}, is the same in both axes, and each grid line involves a separate one dimensional bisection search with accuracy 10^{-6}. Such a solution, obtained for $\nu = 0.25$, is graphically shown in Fig. 2 and the crossing of zero - crossing curves are shown to be on the real axis ($\Omega_2 = 0$). Similar zero crossing curves for complex Poisson's ratio ($0.01 \le \nu_2 \le 0.2$) are given in Fig. 3. The crossing of curves gives the complex solution ($\Omega = \Omega_1 + i\Omega_2$) of the system of equations (27).

To find the solution a refined grid search method along with refinement of search in those squares where are zero crossings of the real and imaginary part of the determinant on their boundaries is used with computation accuracy 10^{-8} [11].

Numerical results were obtained for material properties analogous to those proposed in the literature [8] for the viscoelastic human skull, that is

$$E = 6.895\times10^{10} + i0.092\times10^{3}\ \mathrm{N/m^2}$$
$$\nu = 0.25,\ \text{and}\ \nu = 0.25 + i\nu_2,\ \nu_2:\ \text{variable}$$
$$\rho = 2.132\times10^{3}\left(Kg/m^3\right)$$
$$r_1 = 0.082m,\ \ r_0 \in [0.040, 0.076m]$$

The solution of (27) for real ν corresponds to that of the elastic case which has been presented in Ref. 3 and the results are cited in Table 1. In the case of complex ν, $\nu = 0.25 + i0.1$ and different n (n is the order of Bessel functions) the roots of (27a;b) are given in Table 2. From the results obtained we observe that the ordering of the roots is similar to that of the elastic case and the degeneracy for $n = 1$ disappears. In Table 3 the results for $\nu = 0.25$ and $\nu = 0.25 + i0.1$ are presented. It is observed that the increase in the imaginary part (ω_2) of the first ω for each n follows the decrement of the real part (ω_1).

The dependence of ω_1 and ω_2 on ν_2(ν_1 is constant), is shown in Table 4 and graphically, for the first four eigenfrequencies, in Fig. 4. The variations of ω_1 are small but those of ω_2 are substantially large.

The variations of ω_1^m, ω_2^m, $m = 1,2,3,4$ with h/r_1 ($h = r_1 - r_0$) are shown in Fig. 5. It is observed that ω_1^m, ω_2^m increase with the increment of the skull thickness (for $0 \le h/r_1 \le 0.040$), while for higher values of h/r_1 a decrement is observed for ω_2^m.

4. CONCLUSIONS

In the previous analysis we presented the influence of the viscoelastic nature of the human skull material on its frequency spectrum. From the results obtained we led to the conclusion that for $\nu \in \boldsymbol{R}$ and $E = (\,.\,) + i\,(\,.\,)$ the frequency spectrum of the skull remains almost that of the elastic case and the attenuation is immaterial. For ν and E complex the ordering of the eigenfrequencies remains but there is a decrement of ω_1 and a significant increment of ω_2. We also observed that ω_1^m increases with the increment of the thickness of the skull while there is a critical h beyond of which the attenuation ω_2^m decreases.

Table 1: Frequency spectrum for $\nu = 0.25$ and $r_1 = 0.082m$, $r_0 = 0.076m$.

Elastic Skull		Viscoelastic Skull	
Ω [3]	ω	ω_1	ω_2
0.7083	2709.282	2709.291	18.159
0.8522	3259.638	3259.711	21.849
0.9486	2628.364	3628.446	24.320
1.063	4065.941	4066.033	27.253
1.1971	4578.870	4578.972	30.691
1.2184	4660.341	4660.446	31.237
1.4210	5435.280	5435.402	36.431
1.5479	5920.669	5920.802	39.685
1.6695	6385.785	6385.928	42.802
1.8924	7238.370	7238.533	48.517
2.5324	9686.350	9686.567	64.925
2.6253	10041.689	10041.915	67.307

Figure 2: Solution of (27) in the complex plane (Ω_1, Ω_2) for $\nu = 0.25$, $r_1 = 0.082m$, $r_0 = 0.076m$ and $n = 2$.
(1: $\mathrm{Re}\left[\det\left(D_n^m(\Omega_1,\Omega_2)\right)\right] = 0$, 2: $\mathrm{Im}\left[\det\left(D_n^m(\Omega_1,\Omega_2)\right)\right] = 0$).

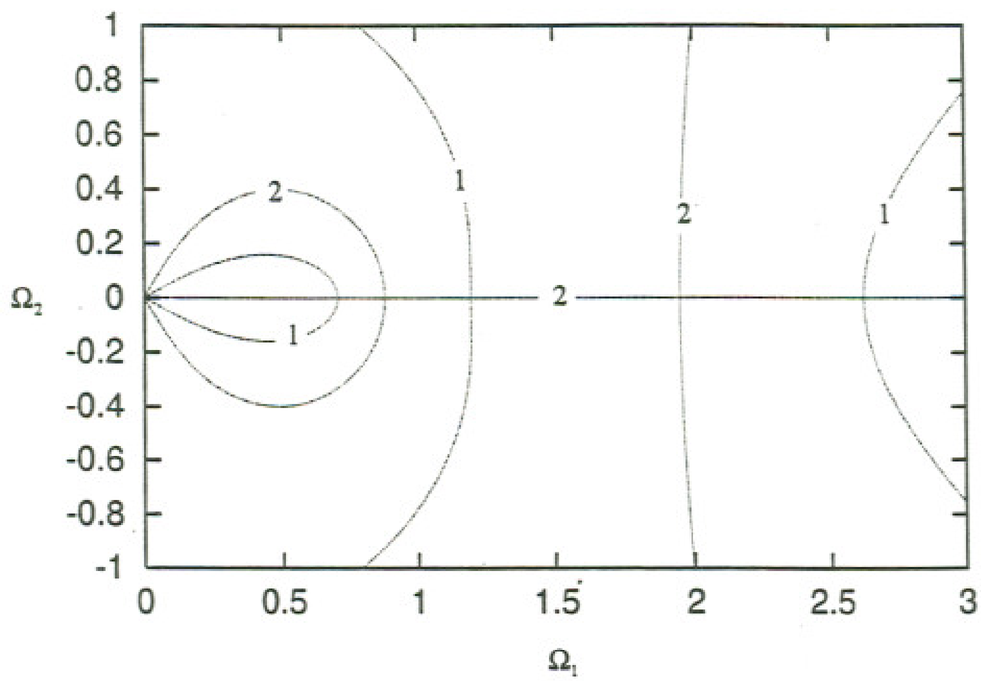

Table 2: Eigenfrequency coefficients $\Omega^{(n)} = \Omega_1^{(n)} + i\Omega_2^{(n)}$, for $\nu = 0.25 + i0.1$, $r_1 = 0.082m$, $r_0 = 0.076m$ and $n = 0,1,\ldots,8$.

	$n=0$		$n=1$		$n=2$		$n=3$		$n=4$		$n=5$		$n=6$		$n=7$		$n=8$	
	Ω_1	$-\Omega_2$	Ω_1	$-\Omega_2$	Ω_1	$-\Omega_2$	Ω_1	$-\Omega_2$	Ω_1	$-\Omega_2$	Ω_1	$-\Omega_2$	Ω_1	$-\Omega_2$	Ω_1	$-\Omega_2$	Ω_1	$-\Omega_2$
1	0	0	0	0														
2					0.7243	0.0792												
3							0.8776	0.0853										
4									0.9770	0.0879								
5											1.0946	0.0922						
6					1.2274	0.1530												
7													1.2539	0.0995				
8															1.4619	0.1010		
9	1.5946	0.0278																
10																	1.7175	0.1252
11							1.9407	0.2418										
12			1.9495	0.1252														
13									2.6037	0.3245								
14					2.7003	0.0904												
15											3.2474	0.4047						
16							3.6207	0.1607										
17													3.8813	0.4837				
18															4.5097	0.5620		
19									4.5881	0.2289								
20																	5.1344	0.6398
21											5.5710	0.2950						
22													6.5603	0.3603				
23															7.5523	0.4256		
24																	8.5455	0.4913

Figure 4: Solution of (27) for $v = v_1 + iv_2$ ($v_1 = const.$) in the complex plane (Ω_1, Ω_2) for $r_1 = 0.082m$, $r_0 = 0.076m$ and $n = 2$. (A: $v_2 = 0.001$, B: $v_2 = 0.01$, C: $v_2 = 0.1$, D: $v_2 = 0.2$)

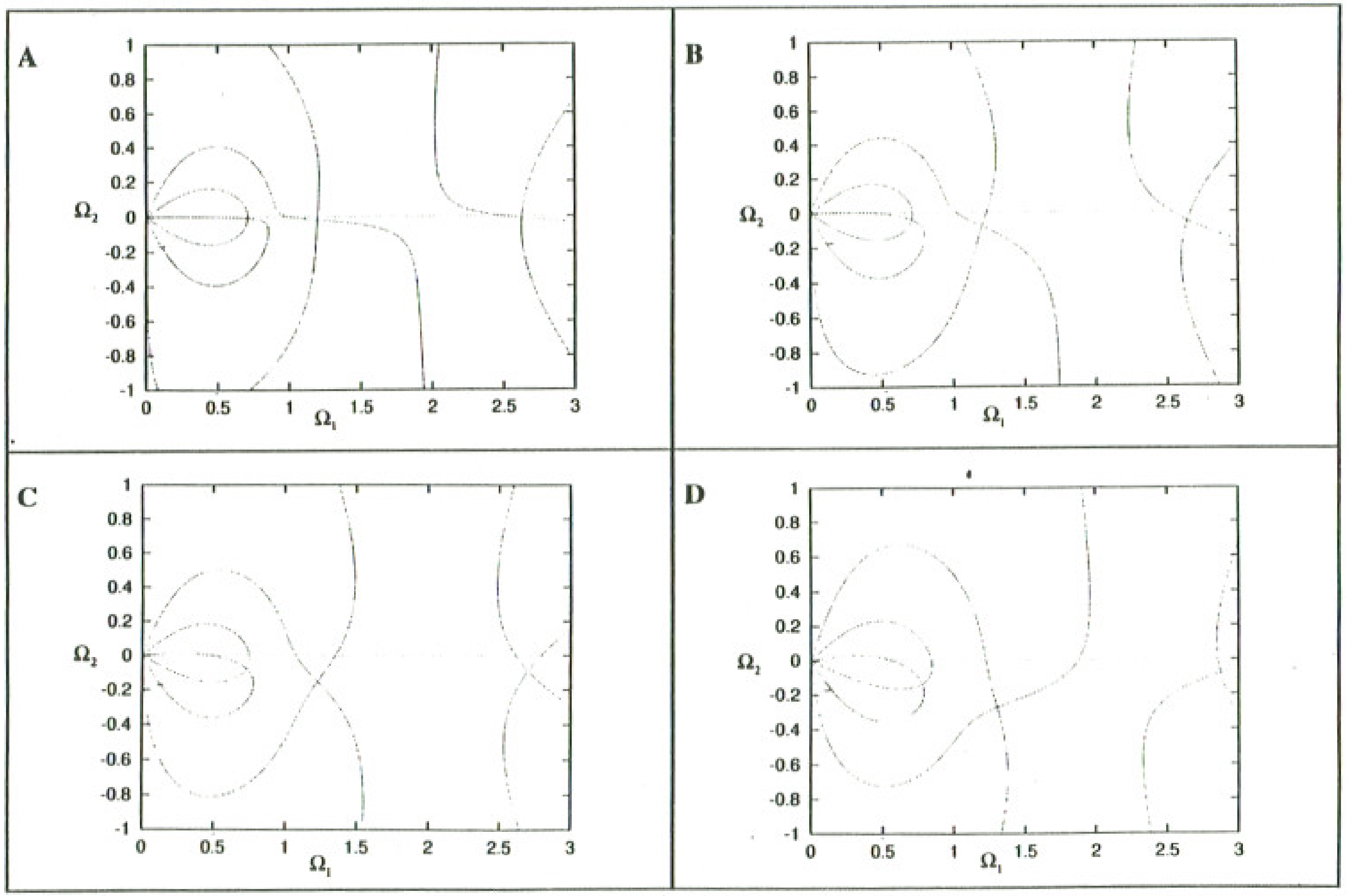

Table 3: Eigenfrequency and attenuation spectra for $\nu = 0.25 + i0.1$ and $r_1 = 0.082m, \ r_0 = 0.076m$.

Elastic Skull [3]		Viscoelastic Skull			
Ω	ω	Ω_1	ω_1	Ω_2	ω_2
0.7083 (n=2)	2784.727	0.7243	2711.926	-0.0792	60.662
0.8522 (n=3)	3355.030	0.8776	3262.434	-0.0853	110.256
0.9486 (n=4)	3735.108	0.9770	3628.634	-0.0879	148.535
1.0631 (n=5)	4184.679	1.0946	4062.345	-0.0922	189.571
1.1971 (n=2)	4692.286	1.2274	4579.019	-0.1530	30.675
1.2184 (n=6)	4793.594	1.2539	4650.483	-0.0995	239.799
1.4210 (n=7)	5588.646	1.4619	5419.097	-0.0110	300.132
1.5479 (n=0)	6096.023	1.5946	5866.431	-0.0278	667.104
1.6695 (n=8)	6565.997	1.7175	6364.619	-0.1252	369.188
1.8924 (n=1)	7452.738	1.9495	7172.260	-0.0345	813.968
1.8924 (n=3)	7419.119	1.9407	7240.025	-0.2418	48.526
2.5324 (n=4)	9953.767	2.6037	9713.487	-0.3245	65.107
2.6253 (n=2)	10323.095	2.7003	9955.172	-0.0904	970.888

Table 4: Eigenfrequency and attenuation spectra for $\nu_2 \in [0.0,\ 0.2]$ and $r_1 = 0.082m,\ r_0 = 0.076m$.

$\nu = 0.25 + i0.01$		$\nu = 0.25 + i0.05$		$\nu = 0.25 + i0.1$		$\nu = 0.25 + i0.15$		$\nu = 0.25 + i0.2$	
ω_1	ω_2	ω_1	ω_2	ω_1	ω_2	ω_1	ω_2	ω_1	ω_2
2709.384	22.430	2728.532	39.479	2711.926	60.662	2715.282	81.527	2719.995	101.955
3259.797	30.720	3284.036	66.158	3262.434	110.256	3266.196	153.956	3271.605	197.043
3628.370	36.791	3655.601	86.613	3628.634	148.535	3629.611	209.747	3631.354	269.933
4066.343	43.579	4096.624	108.755	4062.345	189.571	4058.324	269.092	4053.349	346.764
4579.010	30.693	4607.786	30.692	4579.019	30.675	4579.010	30.691	4579.011	30.695
4660.153	52.241	4694.414	136.072	4650.483	239.799	4639.610	341.427	4625.411	440.309
5435.448	63.018	5474.888	169.073	5419.097	300.132	5400.230	428.193	5375.302	552.007
5919.867	103.033	5906.034	355.641	5866.431	667.104	5803.093	969.904	5726.791	1244.055
6388.110	75.736	6434.002	207.038	6364.619	369.188	6337.188	527.415	6300.660	680.074
7237.320	125.798	7293.849	433.976	7172.260	813.968	7095.609	1183.607	7001.674	1499.185
7240.027	48.528	7295.524	48.529	7240.025	48.526	7240.025	48.528	7240.027	48.527
9713.626	57.460	9774.518	65.099	9713.487	65.107	9713.469	65.105	9713.488	65.110
10040.479	158.562	10114.546	522.437	9955.172	970.888	9854.097	1406.711	9718.613	1824.672

Figure 4: Variation of ω_1^n, ω_2^n, $n = 1,2,3,4$ with ν_2 for $r_1 = 0.082m$, $r_0 = 0.076m$.

	Angular Frequency (ω_1^n)	Attenuation (ω_2^n)
A	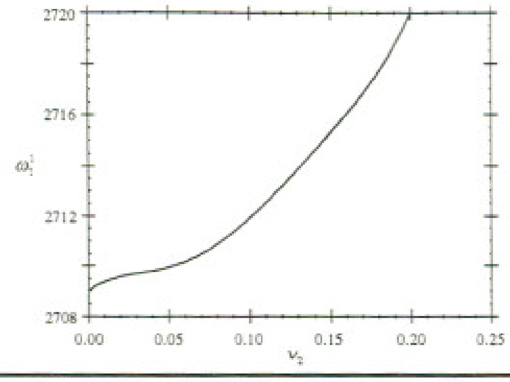	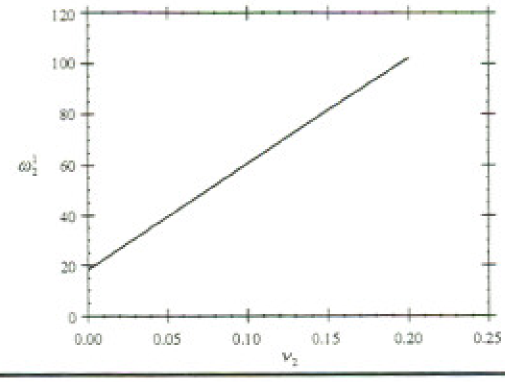
B	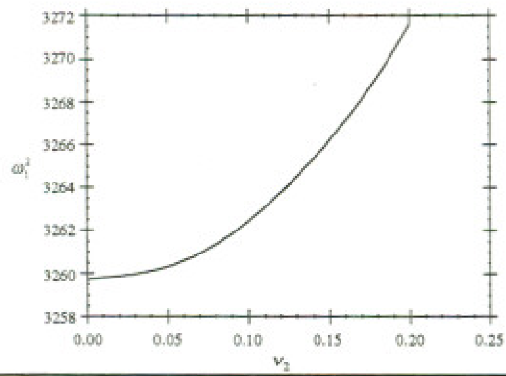	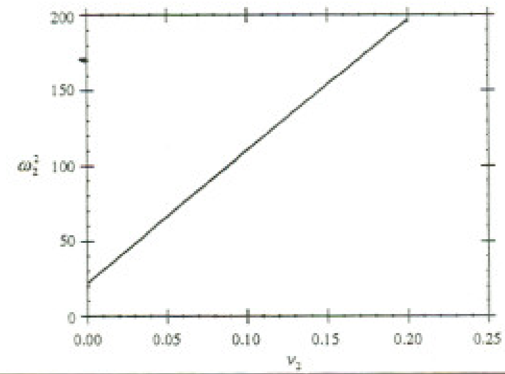
C	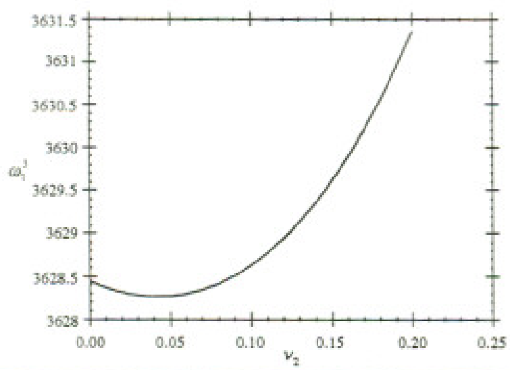	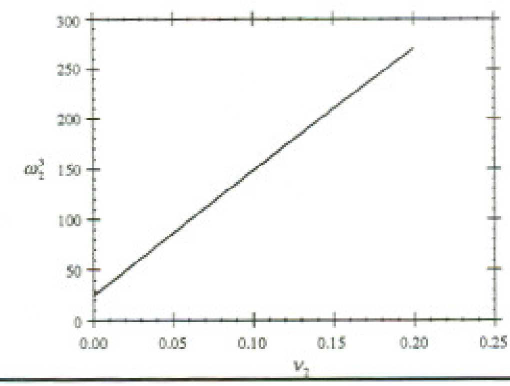
D	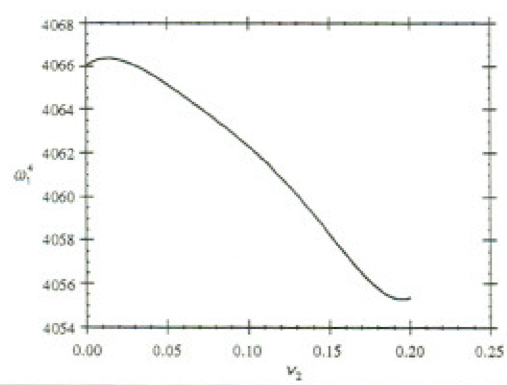	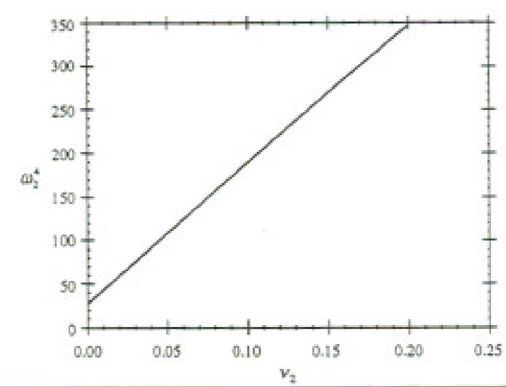

Figure 5: Variation of ω_1^n and ω_2^n with h/r_1 for $\nu = 0.25 + i0.1$ and $r_1 = 0.082m$.

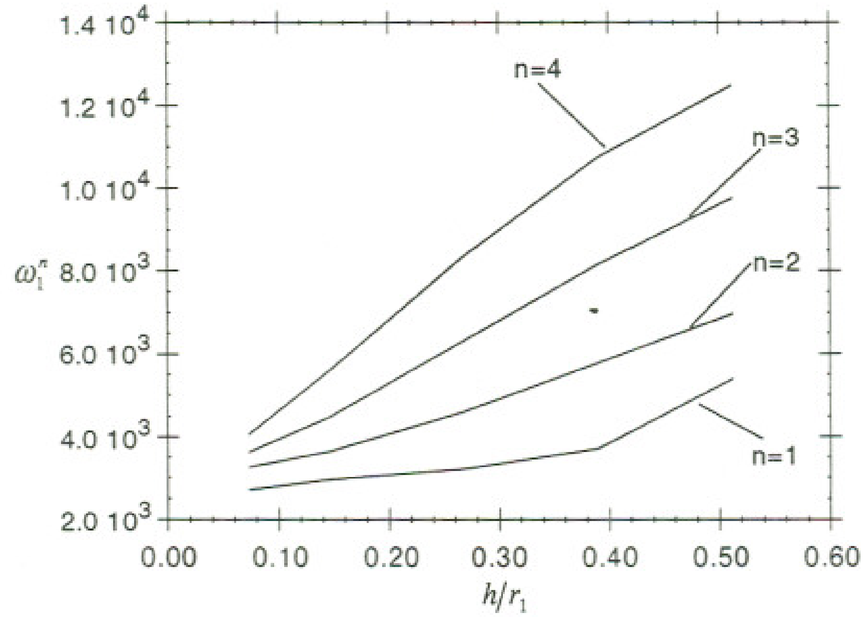

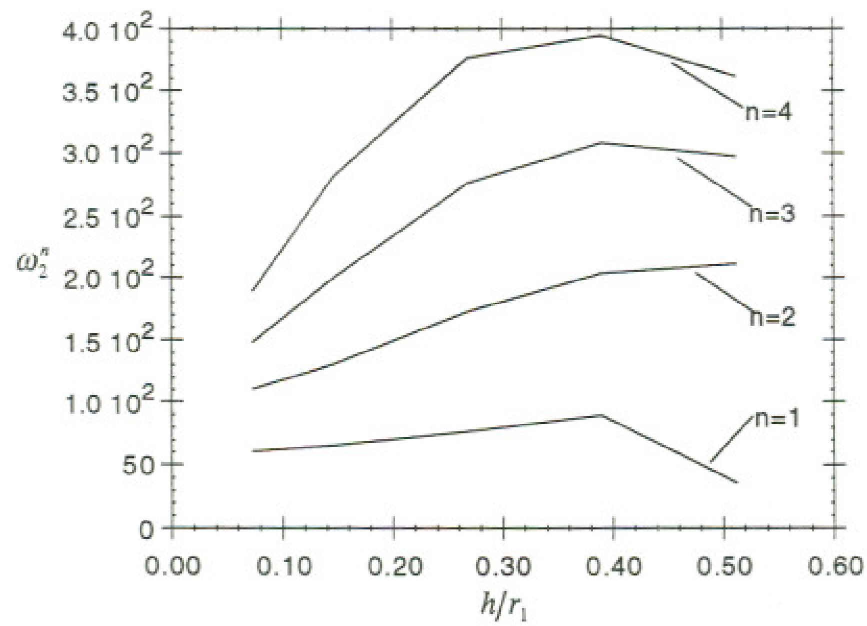

ACKNOWLEDGEMENT

The present work forms part of the project "New Systems for Early Medical Diagnosis and Biotechnological Applications" which is supported by the Greek General Secretariat for Research and Technology through the EU funded R&D Program EPET II.

REFERENCES

[1] T.B. KHALIL, D.C. VIANO and D.L. SMITH, *J. Sound and Vibration* **63**, 351 (1979).

[2] B. HAKANSSON, A. BRANDT and P. CARLSSON, *J. Acoust. Soc. Am.* **95**(3), 1474 (1994).

[3] A. CHARALAMBOPOULOS, G. DASSIOS, D.I. FOTIADIS, V. KOSTOPOULOS, and C.V. MASSALAS, *Int. J. Engng. Sci.* **34**, 1339 (1996).

[4] A. CHARALAMBOPOULOS, D.I. FOTIADIS and C.V. MASSALAS, *Int. J. Engng. Sci.*, accepted (1996).

[5] A. CHARALAMBOPOULOS, D.I. FOTIADIS and C.V. MASSALAS, *Acta Mechanica*, accepted (1997).

[6] J.C. MISRA, *Ingenieur - Archiv* **47**, 11 (1978).

[7] J.C. MISRA and S. CHAKRAVARTY, *J. Biomechanics* **15**, 635 (1982).

[8] R. HICKLING and M.L. WENNER, *J. Biomechanics* **6**, 115 (1973).

[9] W.W. HANSEN, *Phys. Rev.* **47**, 139 (1935).

[10] S. ZHANG and J. JIN, *Computation of Special Functions*, Wiley - Interscience (1996).

[11] G.H. HOSTETTER, M.S. SANTINA, and P. D' CAPRIO - MONTALVO, *Analytical, Numerical, and Computational Methods for Science and Engineering*, Prentice Hall (1991).